Asociación Argentina
de Mecánica Computacional

Mecánica Computacional Vol XXX, págs. 265-276 (artículo completo)
Oscar Möller, Javier W. Signorelli, Mario A. Storti (Eds.)
Rosario, Argentina, 1-4 Noviembre 2011

A PRESSURISED HEAVY WATER REACTOR (PHWR) COOLANT CHANNEL SIMULATION OF THE ATUCHA II NUCLEAR POWER PLANT

Santiago Corzo, Damian Ramajo, Santiago Márquez Damián and Norberto Nigro

International Center for Computational Methods in Engineering (CIMEC), INTEC-UNL-CONICET, Güemes 3450 S3000GLN Santa Fe, Argentina, dramajo@santafe-conicet.gov.ar

Keywords: Coolant channel, pressure loss.

Abstract. The coolant channel components and fuel assembly of the Atucha II PHWR nuclear power plant were simulated. 3D CFD simulation was used for estimating the pressure drop and the flow field around detailed models of one of the spacers and the channel outlet throttle port. Results allow for a deep understanding of the channel flow and the frictional and form pressure losses inside the channel. Results were compared with experimental data for a simplified spacer and correlations for the pressure drop from literature were also implemented obtaining good agreement.

1 INTRODUCTION

The core cooling channels of the Pressure Water Reactor (PHWR) Atucha II have a vertical configuration of 451 channels located in the moderator vessel. Each one of this has the aim to remove the thermal energy generated by fission of atoms through a coolant flow pumped under high pressure from the lower-plenum to the upper-plenum. The fuel bundles are composed by a set of 37 fuel rods of 5.3 m active length with 13 spacers to strength the fuel assembly.

The total pressure drop along the coolant channels include the inlet flow restrictors at the lower ends and outlet throttles at the upper ends, the friction losses along the fuel rods, and the form losses due to the presence of spacers. The entrance losses are those due to a sudden change in flow area (not contemplated in this study). Hence the attention is focused on the friction along the rod bundles and the effect of spacers throttles.

The main objective of this study is to present profiles of pressure losses in Atucha II fuel bundles, particularly in fuel rod spacers and throttles zones performing a comparative study of the existing correlations. These zones present localized pressure drops due to cross section sudden changes plus the frictional losses. The negative feature of spacer grids is the introduction of considerable pressure losses in fuel assemblies.

2 MATHEMATICAL FORMULATION

The model is based on Newtonian incompressible flow with dynamic and thermo-physical properties assumed to be constant. Steady-state simulations were performed using ANSYS CFX 13. The governing equations (see Equations 1-4) were solved with a pressure based solver:

$$\frac{\partial v_x}{\partial x}+\frac{\partial v_y}{\partial y}+\frac{\partial v_z}{\partial z}=0 \qquad (1)$$

$$v_x\frac{\partial v_x}{\partial x}+v_y\frac{\partial v_x}{\partial y}+v_z\frac{\partial v_x}{\partial z}=-\frac{1}{\rho}\frac{\partial p}{\partial x}+\nu\left(\frac{\partial^2 v_x}{\partial x^2}+\frac{\partial^2 v_x}{\partial y^2}+\frac{\partial^2 v_x}{\partial z^2}\right) \qquad (2)$$

$$v_x\frac{\partial v_y}{\partial x}+v_y\frac{\partial v_y}{\partial y}+v_z\frac{\partial v_y}{\partial z}=-\frac{1}{\rho}\frac{\partial p}{\partial y}+\nu\left(\frac{\partial^2 v_y}{\partial x^2}+\frac{\partial^2 v_y}{\partial y^2}+\frac{\partial^2 v_y}{\partial z^2}\right) \qquad (3)$$

$$v_x\frac{\partial v_z}{\partial x}+v_y\frac{\partial v_z}{\partial y}+v_z\frac{\partial v_z}{\partial z}=-\frac{1}{\rho}\frac{\partial p}{\partial z}+\nu\left(\frac{\partial^2 v_z}{\partial x^2}+\frac{\partial^2 v_z}{\partial y^2}+\frac{\partial^2 v_z}{\partial z^2}\right) \qquad (4)$$

3 DROP PRESSURE MODEL IN FUEL BUNDLES

The model consists only in a middle section channel of length 455 mm (Figure 1) due to the cross longitudinal symmetry. The domain was meshed using a total of 4.674.284 elements with 3.173.879 tetrahedrons and three hexahedron layers with 1.458.447 elements near the walls. The mesh size was chosen based on a convergence mesh analysis to find a goal mesh size and distribution that ensure an accurate pressure drop for the maximum mass flow rate.

Respect to mesh convergence tests, we do not report results in this work and we only limit ourselves to conclude that the mesh mentioned above has the correct distribution of cells close to the walls, allowing to obtain good agreement with the empirical correlations.

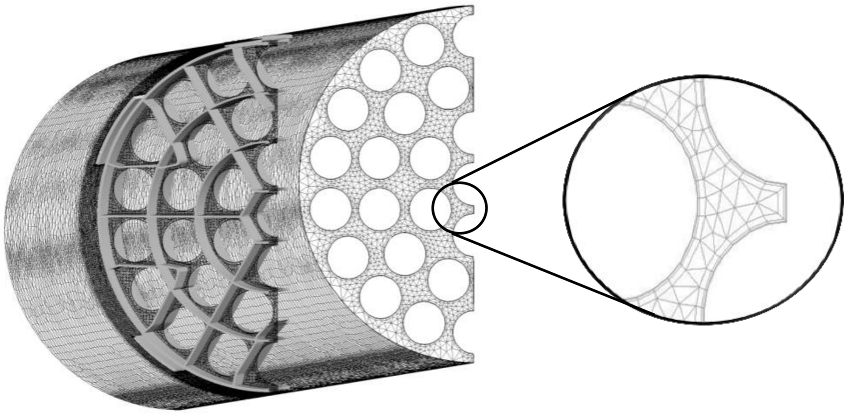

Figure 1: Geometry and mesh details

The pressure losses in the fuel assembly with one spacer consist of the friction pressure losses in rod bundle and the local pressure loss at the spacer grid. For a bare rod bundle the friction pressure loss can be calculated from the Darcy–Weisbach expression as shown below (Moskva and Leningrad, 1960):

$$\Delta p = \lambda \frac{1}{2} \rho v^2 \left(\frac{L}{Dh}\right) \quad (5)$$

Where: λ is the Darcy friction factor, L the length and Dh the hydraulic diameter.

A commonly used correlation for the turbulent friction factor is the Colebrook equation (Truckenbrodt, 1968):

$$\frac{1}{\sqrt{\lambda_{tur}}} = -2 \log\left[\frac{2.51}{Re\sqrt{\lambda_{tur}}} + 0.27\frac{r}{Dh}\right] \quad (6)$$

To avoid the necessity of using an iterative procedure to solve the above equation, an estimation for the friction coefficient for laminar flow λ_l on the right hand side is used:

$$\frac{1}{\sqrt{\lambda_l}} = -2 \log\left[\frac{r}{3.7Dh} + \left(\frac{6.81}{Re_l}\right)^{0.9}\right] \quad (7)$$

The Lehmann´s friction coefficient is calculated based on the following equation:

$$\frac{1}{\lambda_{tur}} = 1.94 \log\left\{\left[\left(\frac{4.26}{Re}\right)(\lambda_{tur})^{-0.5}\right]^{1.1} + \left[\frac{1}{3.71}\left(\frac{r}{Dh}\right)\right]^{1.03}\right\} \quad (8)$$

Other empirical correlation that can be used was provided by Cheng and Todreas (Cheng and Toedras, 1986):

$$\lambda_{tur} = \frac{0.17}{\mathrm{Re}^{0.18}} \quad (9)$$

The first set of cases modeled was carried out using different mass flow rates at the inlet. The constants and parameters for these simulations were as follows (Table1)

	Value
Roughness (μm)	5
Temperature (ºC)	306.0
Density (kg/m³)	702.11
Dynamic viscosity (Pa s)	8.457×10^{-5}

Table 1: Geometric details of the fuel bundle.

Simulations were carried out, with high order discretization scheme for momentum equation and first order upwind for turbulent quantities ANSYS CFX solver guide. This code is based on the control volume method using a Semi-implicit method for pressure-linked equations (SIMPLE) algorithm to the pressure-velocity coupling. k-epsilon was used as the close model for momentum equation. Scaled residuals were below 1×10^{-5}.

Once convergence was obtained the pressure drop was measured along 12 axial probe lines. The position of these lines has the aim of obtain information about variability in pressure losses due to the geometrical differences and cross sectional area transitions. Figure 2 shows the pressure drop distribution averaged among all probe lines for different mass flow rates.

To estimate the pressure drop by friction it was computed the turbulent friction factor using the Darcy–Weisbach equation and then it was compared with other empirical correlations (see Table 2). To obtain the pressure drop a portion of the channel were the local influence of the spacer does not affect the free stream flow was chosen. Figure 2 shows the two test sections (dotted lines) enclosing a 200mm length of the rod bundle. In this zone the total averaged pressure difference was obtained. Results show how the static pressure recovers a part of its original value downstream of the spacer. With respect to the total pressure, Figure 2.a shows a particular behavior increasing total pressure at the spacer inlet especially for the highest turbulent regimes. This effect could be explained by the high velocity gradient where flow have to change the direction and flow velocity is over-predicted.

Mass flow rate (kg/sec)	Re	f	f (Colebrook)	f (Lehmann)
21.52	585420	0,01621	0,0175	0,0174
15.70	427130	0,01650	0,0178	0,0176
12.59	340090	0,01674	0,018	0,0179
9.30	253030	0,01721	0,0184	0,0182

Table 2: Turbulent friction factor.

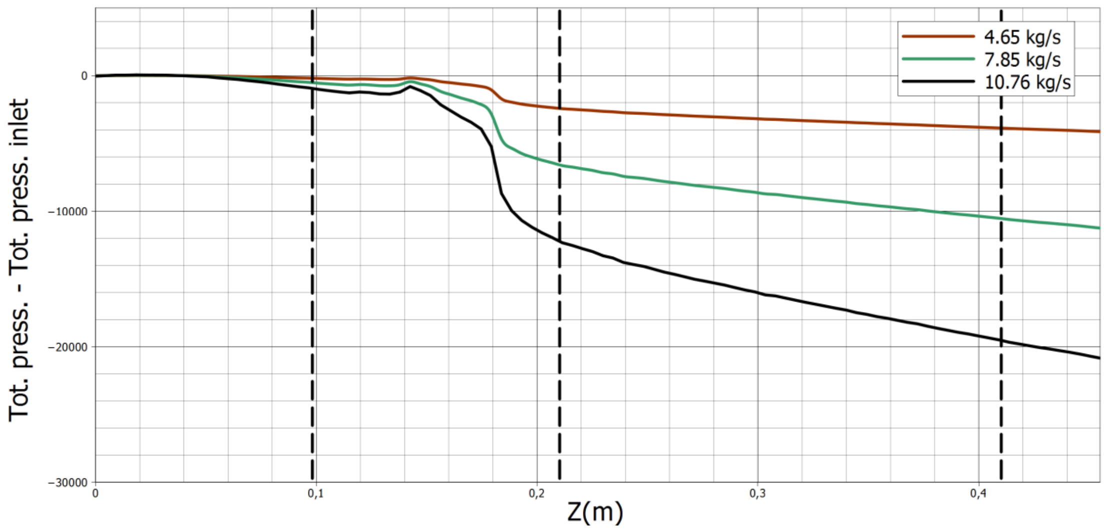

a)

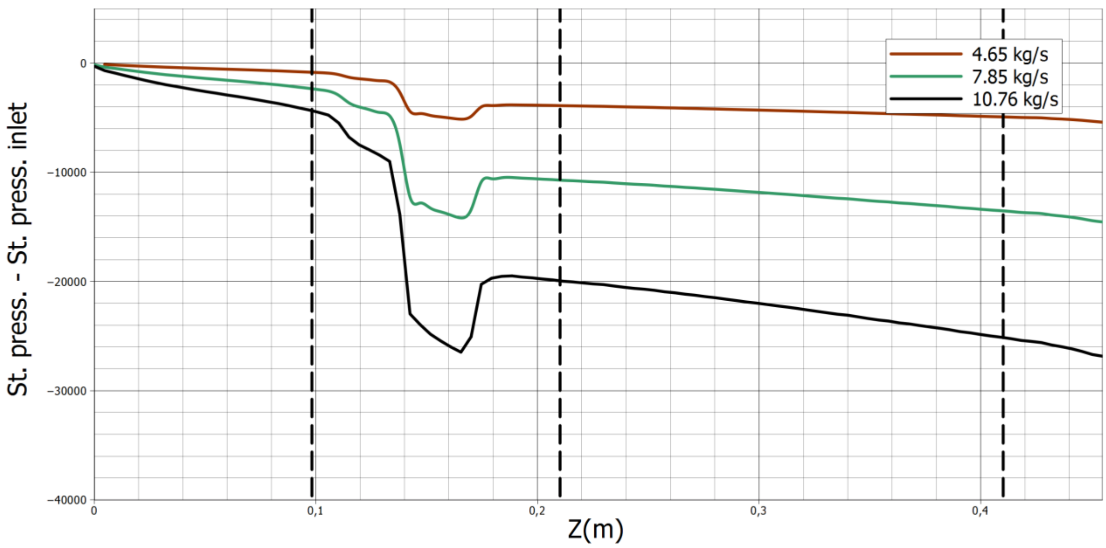

b)

Figure 2: Pressure distribution along fuel assembly for different mass flow rates. a) Total pressure; b) static pressure.

The maximum error obtained respect to the empirical correlations was approximately 7% corresponding to the minimum mass flow (see Figure 3). This slight discrepancy leds to the realization of a second series of tests. In this new series the roughness variation on the diverse surfaces and its influence in the pressure drop was studied. So, this study was carried out with the parameters summarized in Table 3.

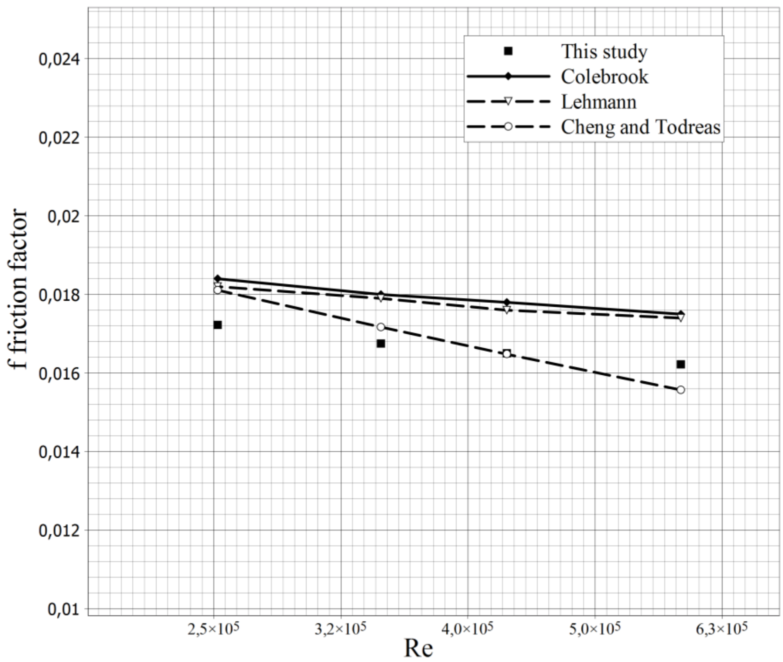

Figure 3: Friction factor

	Roughness (μm)			Mass flow rate (kg/sec)
	Fuel rods	Channel wall	Spacer	
Test 1	16	16	16	21.52
Test 2	5	16	16	21.52
Test 3	5	5	16	21.52
Test 4	5	5	5	21.52

Table 3: Case variation.

Figure 4 shows the effect of each wall rough tested.

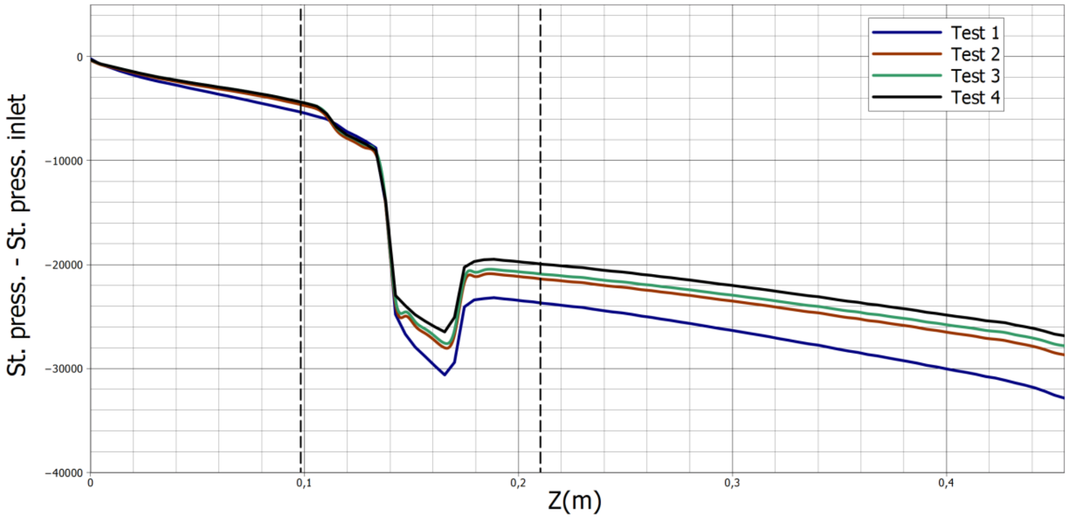

a)

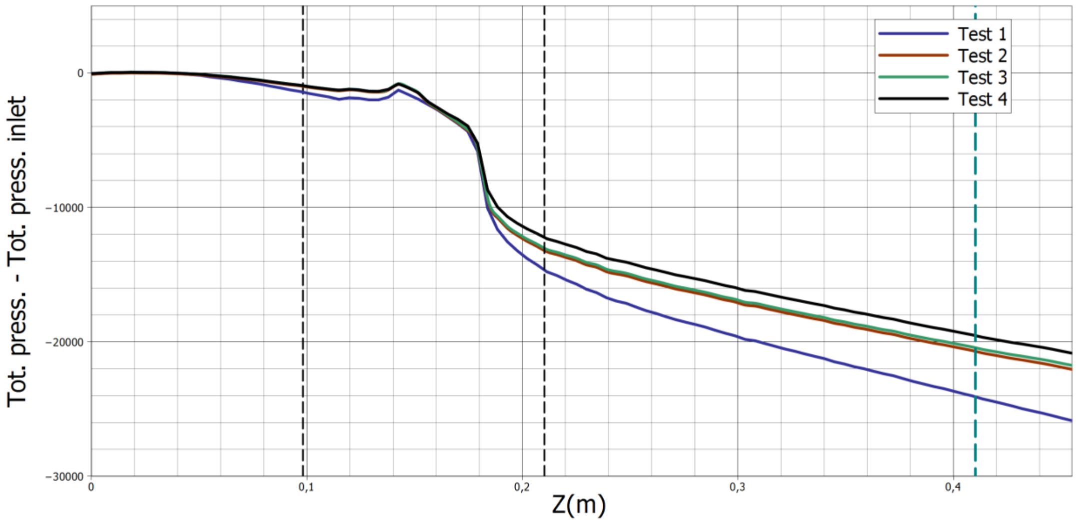

b)

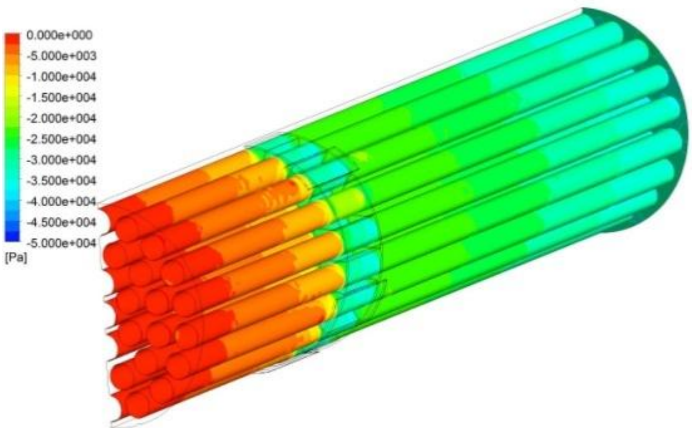

c)

Figure 4: Pressure distribution along fuel assembly: a) and b): Differences due to wall roughness, Averaged static pressure and Averaged total pressure along probe lines respectively; c) Contour of static pressure showed over the fuel bundle geometry.

Regarding to the form loss pressure in the spacer zone, he pressure drop is computed pressure in the local zone between dotted lines as was shown in Figure 4. The choosing criterion for this zone was to select the closest points from spacer to free stream. The form losses factor in the spacer zone estimated are presented in Figure 5.

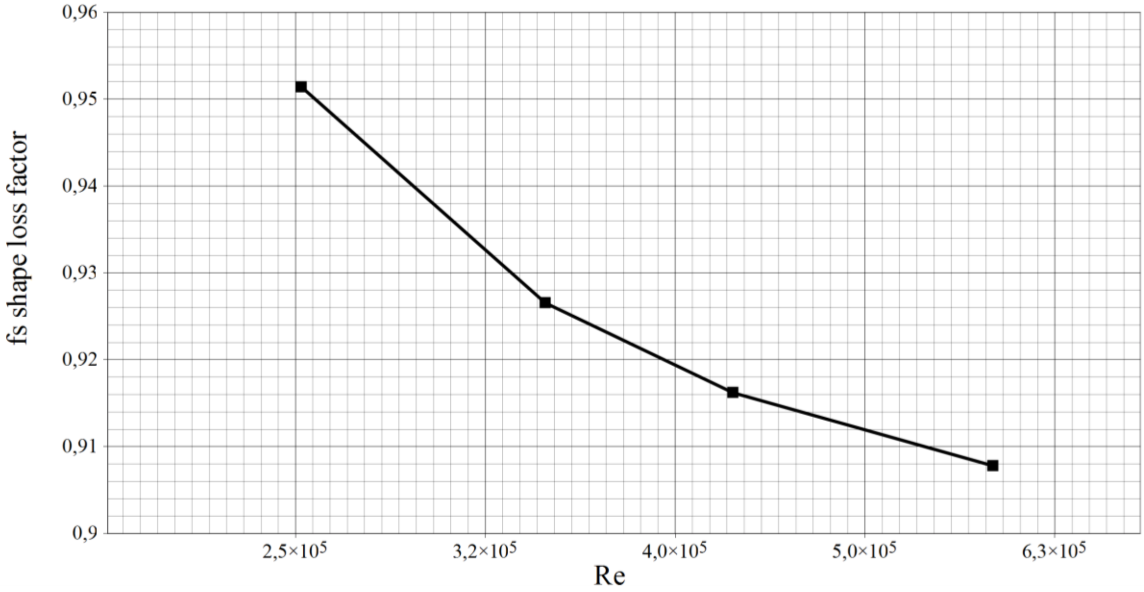

Figure 5: Spacer form factor vs. Re numbers

All experimental studies in this sense were carried out using pure water as the fluid. For this reason the above models were simulated with the same fluid. To contemplate differences in pressure losses using heavy water or light water a comparative study was also done. The heavy water properties are included in Table 4.

	Value
Roughness(μm)	5
Temperature (ºC)	306.0
Density(kg/m^3)	$796_{(+10\%)}$
Dynamic viscosity(Pa s)	$1.085\text{x } 10^{-4}{}_{(+25\%)}$
Mass flow rate(kg/sec)	9.3

Table 4: Geometric details of the fuel bundle

Figure 7 shows these results. Under equal boundary conditions, heavy water presents less pressure drop with respect to light water in the core cooling channel.

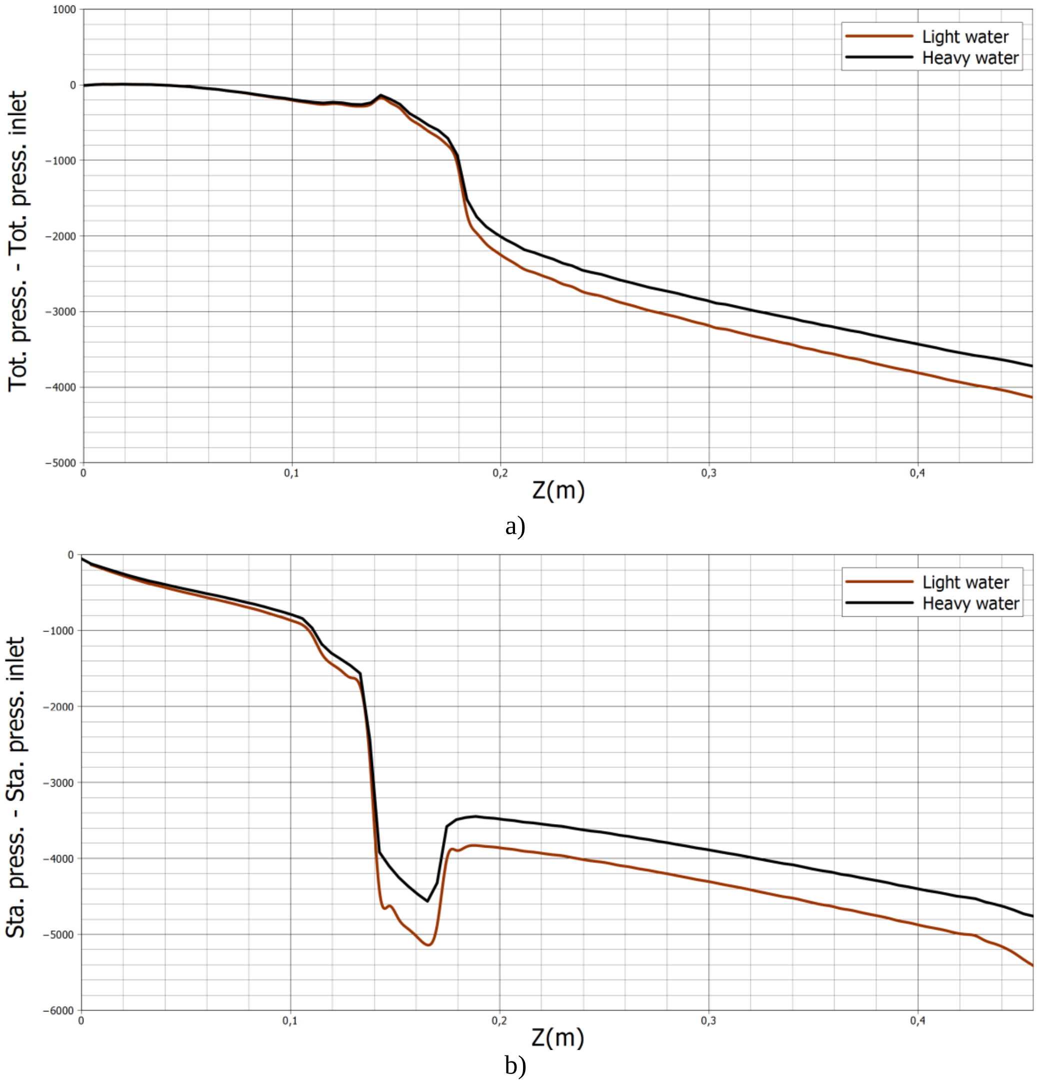

Figure 6: Pressure distribution for different fluids along fuel bundles. a) Static pressure; b) Total pressure.

4 DROP PRESSURE MODEL IN THROTTLES OF THE CHANNEL FUEL BUNDLES

The problem addressed in this section deals with the numerical simulation of the drop pressure in the channel outlet where the fluid pass through the support bars zones until the upper plenum zone. The geometry (See Figure 8) was meshed with same criteria that the previous model. The mesh size is 6.350.000 elements and its domain is only extended to a section of the upper plenum together with the last stretch of the channel. The model has the same parameters as the previous cases. Steady-state pressure based solver. High order discretization scheme for the momentum equation and first order upwind for turbulent quantities. k-epsilon was used as the turbulent model for momentum equation. Scaled residuals were below 1 10^{-5}.

Figure 8 shows the measurement planes where the averaged pressure was computed. For the present fluid-dynamic behavior (drop pressure – mass flow rate) the simulation was carried out with different mass flow rate at inlet. The parameters are summarized in Table 5.

	Value
Roughness (µm)	5
Temperature (ºC)	306.0
Density (Kg/m^3)	702.11
Dynamic viscosity (Pa s)	8.457e-05
Mass flow rate (kg./sec.)	see table 2

Table 5: Details of the fuel bundle

The results obtained are presented in Table 6. Form loss factor is computed on the throttles zones using Darcy–Weisbach (5) equation.

Mass flow rate (kg/sec)	*f* Planes 5-11	*f* Planes 10-11
27.73	1.376	0.282
21.27	1.349	0.266
15.08	1.361	0.273
11.70	1.355	0.267
9.29	1.364	0.276

Table 6: friction factor.

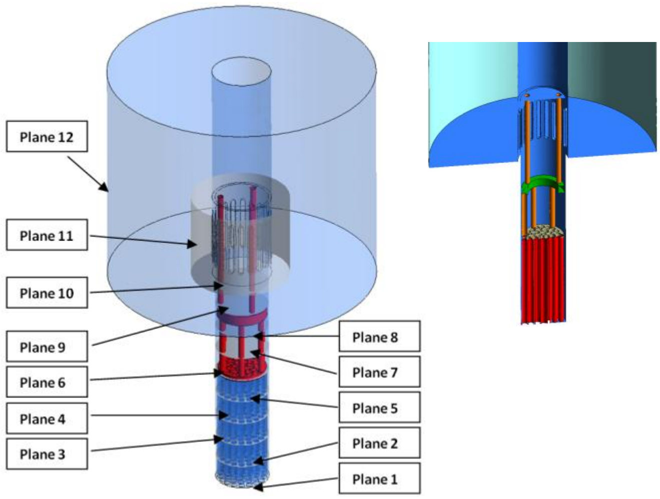

Figure 7: Geometry details for fuel channel throttles

In view of the results, Table 6 shows how the form losses factor do not vary respect to the mass flow (or Re number) as expected. This is evident in Figure 8 where the total pressure varies in the same way between planes with local obstructions unlike the planes where the drop pressure correspond to the friction. These results cannot be compared with other researches due that does not exist previous antecedent of similar works.

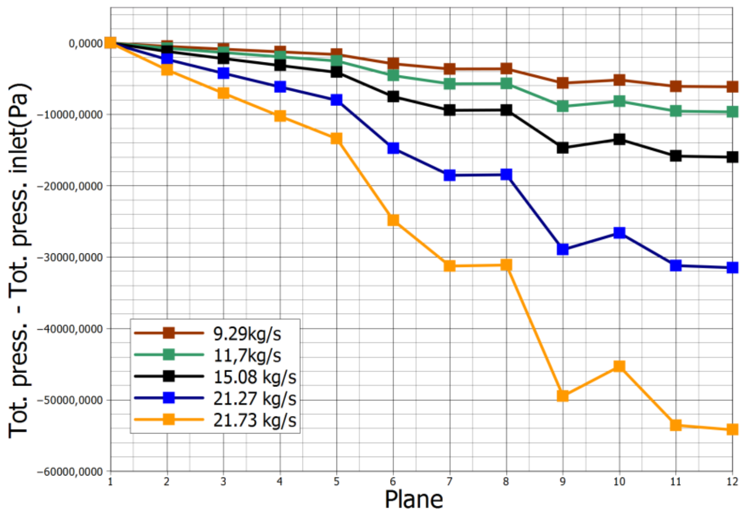

a)

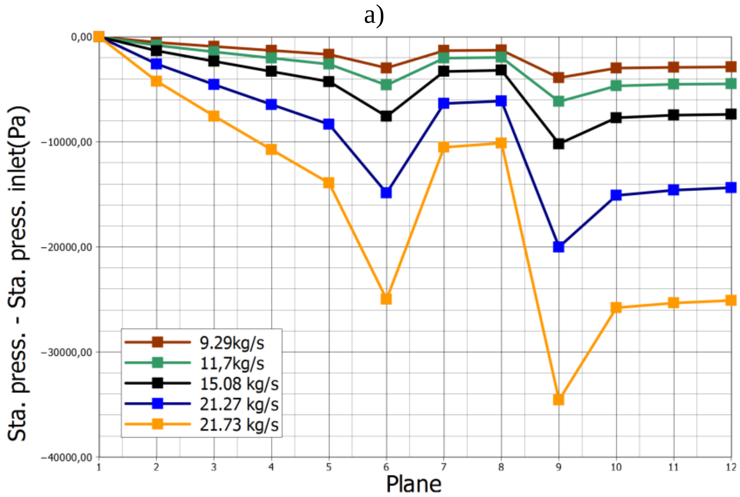

b)

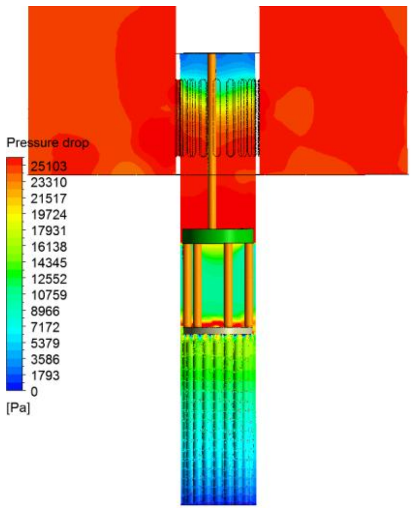

c)

Figure 8: Pressure distribution in fuel channel throttles a) Total pressure; b) Static pressure; c) Contour of static pressure shown over fuel channel throttles geometry.

5 CONCLUSIONS

In view of the results presented above we conclude that the models applied present good agreement with empirical correlations to estimate the pressure drop across various components of PHWR fuel channel. To achieve good results in the spectrum of turbulent regime analyzed in this study using numerical methods is not a simple task, specially due to mesh requirements for both form and frictional pressure losses. These results were checked against experimental results using simplified spacers and showed great agreement (experimental data cannot be exhibited by privacy policies).

For this reason this research may be used to estimate the total pressure drop under single phase condition fluid along the most important zone under a Loss of Coolant Accident (LOCA).

REFERENCES

Cheng, S.K., Todreas, N.E., Hydrodynamic models and correlations for bare and wire-wrapped hexagonal rod bundles-bundle friction factors, subchannel friction factors and mixing parameters. *Nuclear Engineering and Design*, 227±251,1986.

Moskva, Leningrad, Handbook of Hydraulic Resistance. *Goudarstvennoe Energeticheskoe Izdatel´stvo*, 1960.

Truckenbrodt, E., Strömungsmechanik. *Springer Verlag Berlin, Heidelberg, NewYork,* 1968.